

ARSENOPYRITE MELTING DURING METAMORPHISM OF SULFIDE ORE DEPOSITS

ANDREW G. TOMKINS[§]

Department of Geology and Geophysics, University of Calgary, Calgary, Alberta T2N 1N4, Canada

B. RONALD FROST

Department of Geology and Geophysics, University of Wyoming, Laramie, Wyoming 82071, USA

DAVID R.M. PATTISON

Department of Geology and Geophysics, University of Calgary, Calgary, Alberta T2N 1N4, Canada

ABSTRACT

Arsenopyrite is present as a minor phase in many different types of ore deposits. Here we investigate a number of ore deposits metamorphosed to mid-amphibolite facies and above to show that in some environments, arsenopyrite is likely to melt during metamorphism, but in others it will persist until it is converted to löllingite + pyrrhotite. The fate of arsenopyrite is governed by the sulfur fugacity imposed by the surrounding mineralogy during metamorphism. At the Hemlo gold deposit, Canada, which contains a range of disseminated sulfides, the breakdown of barite promoted conditions of high $f(S_2)$ and melting of arsenopyrite during prograde metamorphism. On the other hand, at several massive sulfide deposits including Osborne Lake, Montauban and Geco in Canada, high $f(S_2)$ conditions were instead generated through pyrite breakdown on the pyrite–pyrrhotite buffer, also causing arsenopyrite to melt in favorable parts of the deposits. In contrast, metamorphic processes that inhibit high $f(S_2)$ through consumption of sulfur promote the solid-state conversion of arsenopyrite to löllingite and pyrrhotite rather than melting. In most mineral deposits, the strongest influence on sulfur fugacity is the pyrite-to-pyrrhotite reaction, which buffers $f(S_2)$ to increasingly elevated values as temperature increases. Once pyrite is consumed, however, $f(S_2)$ no longer is maintained at elevated values. If rocks hosting arsenopyrite are able to conserve pyrite to middle-amphibolite-facies conditions (beyond 491°C at 1 bar, or ~560°C at 5 kbar), arsenopyrite melting will occur. If not, arsenopyrite melting is unlikely, though still possible. Of the mechanisms that promote pyrite decomposition at metamorphic conditions below arsenopyrite melting, sequestration of sulfur by iron silicates or oxides (or both) to form pyrrhotite may be the most effective in many types of deposit. At the Calumet deposit and in some parts of the Geco deposit, this process was found to be effective in converting pyrite to pyrrhotite in magnetite-rich rocks. Pyrite consumption and low- $f(S_2)$ conditions are also promoted to a small extent by incorporation of sulfur in hydrothermal fluids, such as an introduced fluid or those generated by dehydration reactions, this effect becoming more significant as temperature rises. Deposits where arsenopyrite is likely to melt during metamorphism include pyrite-rich massive sulfide deposits as well as disseminated deposits lacking abundant iron silicates and oxides. The As-rich melts that result are highly effective in incorporating and mobilizing other metals, particularly gold and silver, as demonstrated at the Challenger deposit (Australia) and at Hemlo, Ontario.

Keywords: arsenopyrite, sulfide melt, metamorphism, ore deposits, mobilization, gold.

SOMMAIRE

L'arsénopyrite est présente en quantités mineures dans plusieurs sortes de gîtes minéraux. Nous examinons ici quelques gisements ayant subi un degré de métamorphisme au faciès amphibolite moyen ou à un faciès plus élevé, afin de montrer que dans certains milieux, l'arsénopyrite est apte à fondre au cours du métamorphisme, quoique dans d'autres, elle peut persister jusqu'au point où elle se déstabilise pour former löllingite + pyrrhotite. Son sort dépend de la fugacité du soufre imposée par l'assemblage de minéraux dans le milieu pendant le métamorphisme. Dans le gisement d'or de Hemlo, en Ontario, dans lequel on trouve une variété de sulfures disséminés, la déstabilisation de la barite provoque une fugacité élevée du soufre, et la fusion de l'arsénopyrite lors du métamorphisme prograde. Par ailleurs, à plusieurs autres gisements de sulfures massifs, par exemple ceux de Osborne Lake, Montauban et Geco au Canada, les conditions de $f(S_2)$ élevée sont apparues à cause de la déstabilisation de la pyrite en traversant le tampon pyrite–pyrrhotite, et ont aussi mené à la fusion de l'arsénopyrite dans les parties favorables de ces gisements. En revanche, les processus métamorphiques qui empêchent la hausse de la fugacité de soufre causeront la perte

[§] *Present address:* School of Geosciences, Monash University, P.O. Box 28E, Melbourne, Victoria 3800, Australia. *E-mail address:* andy.tomkins@sci.monash.edu.au

de soufre pour promouvoir la conversion à l'état solide de l'arsénopyrite en löllingite et pyrrhotite plutôt que la fusion. Dans la plupart des gîtes minéraux, l'influence la plus forte sur la fugacité du soufre est la réaction de pyrite à pyrrhotite, qui tamponne la valeur de $f(S_2)$ à des niveaux toujours plus élevés à mesure qu'augmente la température. Une fois la pyrite éliminée, toutefois, la valeur de $f(S_2)$ n'est plus maintenue à un niveau élevé. Si les roches contenant l'arsénopyrite peuvent conserver la pyrite jusqu'aux conditions du faciès amphibolite moyen (au delà de 491°C à 1 bar, ou ~560°C à 5 kbar), on peut s'attendre à voir fondre l'arsénopyrite. Sinon, il est peu probable que l'arsénopyrite puisse fondre, quoique la possibilité existe toujours. Parmi les mécanismes qui promeuvent la déstabilisation de la pyrite à des conditions métamorphiques en dessous des conditions de fusion de l'arsénopyrite, l'incorporation du soufre par des silicates ou des oxydes de fer (ou les deux) pour former la pyrrhotite pourrait bien être le moyen le plus efficace dans plusieurs types de gisement. Dans le cas du gisement de Calumet et dans certaines parties du gisement de Geco (les deux au Canada), ce processus s'avère efficace dans la conversion de pyrite en pyrrhotite dans les roches riches en magnétite. L'élimination de la pyrite et l'établissement des conditions de faible $f(S_2)$ seraient aussi favorisés à un degré moindre par la répartition du soufre dans un fluide hydrothermal, par exemple une phase fluide introduite ou bien générée par une réaction de déshydratation, cet effet revêtant une importance plus grande à mesure qu'augmente la température. Parmi les gisements dans lesquels l'arsénopyrite est disposée à fondre au cours du métamorphisme, notons les gisements de sulfures massifs riches en pyrite et les gisements disséminés dépourvus de silicates et d'oxydes de fer répandus. Les liquides riches en arsenic qui peuvent apparaître seront très efficaces pour incorporer et mobiliser certains autres métaux, en particulier l'or et l'argent, comme le démontrent le gisement de Challenger en Australie, et celui de Hemlo, en Ontario.

(Traduit par la Rédaction)

Mots-clés: arsénopyrite, bain fondu sulfuré, métamorphisme, gîte minéral, mobilisation, or.

INTRODUCTION

Arsenic-bearing sulfide melts are recognized to have formed during metamorphism in a number of different ore deposits (Hofmann 1994, Tomkins & Mavrogenes 2002, Frost *et al.* 2002a, Tomkins *et al.* 2004). Furthermore, it has been suggested that gold and other metals may be sequestered by these As-bearing melts, making recognition of the controls and behavior of these melts of economic importance. The arsenic in these melts could come from the breakdown of several minerals, the most common being arsenopyrite, tennantite, realgar and orpiment. Of these, orpiment, realgar and tennantite melt at 310°, 318° and 665°C, respectively (at 1 bar; Massalski *et al.* 1990, Maske & Skinner 1971), but a temperature increase alone is not enough to induce melting of arsenopyrite. The stability of arsenopyrite also depends on sulfur fugacity (Barton 1969), and thus also on related chemical parameters such as oxygen fugacity.

Tomkins *et al.* (2004) showed sulfide melts to be highly mobile during deformation. Thus, there is potential for segregation of these melts, possibly leading to new metal-rich accumulations. Melting of arsenopyrite may be critical to the early onset of melting in massive sulfide deposits (Frost *et al.* 2002a); without it, melting may not occur in these deposits until the granulite facies is reached. In addition, because arsenopyrite is commonly associated with gold, it is important to understand the physical and chemical processes that lead to or inhibit the melting of arsenopyrite during metamorphism.

Experiments in the system Fe–As–S were first conducted by Clark (1960a, b), who recognized that arsenopyrite could melt during amphibolite-facies metamorphism. However, Barton (1969) showed that the stability of arsenopyrite is dependent on $f(S_2)$.

Improvements on the understanding of the stability field of arsenopyrite in log $f(S_2)$ –T–P space were subsequently made by Kretschmar & Scott (1976) and Sharp *et al.* (1985). In this study, we review the metamorphic reactions by which melting of arsenopyrite can occur, as well as reactions that inhibit melting. Geological environments where some of these reactions may have taken place are then discussed.

METAMORPHIC REACTIONS RELEVANT TO ARSENOPYRITE MELTING

Arsenopyrite typically coexists in ore deposits with other sulfide minerals. Pyrite or pyrrhotite (or both) are almost invariably present, and it is these two minerals that are likely to control the stability of arsenopyrite during metamorphism in most deposits. Therefore, in this section we first review metamorphic processes that affect the stability of pyrite and pyrrhotite, so that we can then address the stability of arsenopyrite from the perspective of whole-rock composition.

The system Fe–S

The simplest desulfidation-type reaction that proceeds during prograde metamorphism of a sulfide ore deposit is one that has been recognized for many years, that of pyrite breaking down to form pyrrhotite (Toulmin & Barton 1964, Craig & Vokes 1993; Fig. 1):



Because pyrite is common in many sulfide deposits, reaction (1) exerts the major influence on $f(S_2)$ conditions during metamorphism. This reaction is referred to as the pyrite–pyrrhotite (Py–Po) buffer because $f(S_2)$ –T

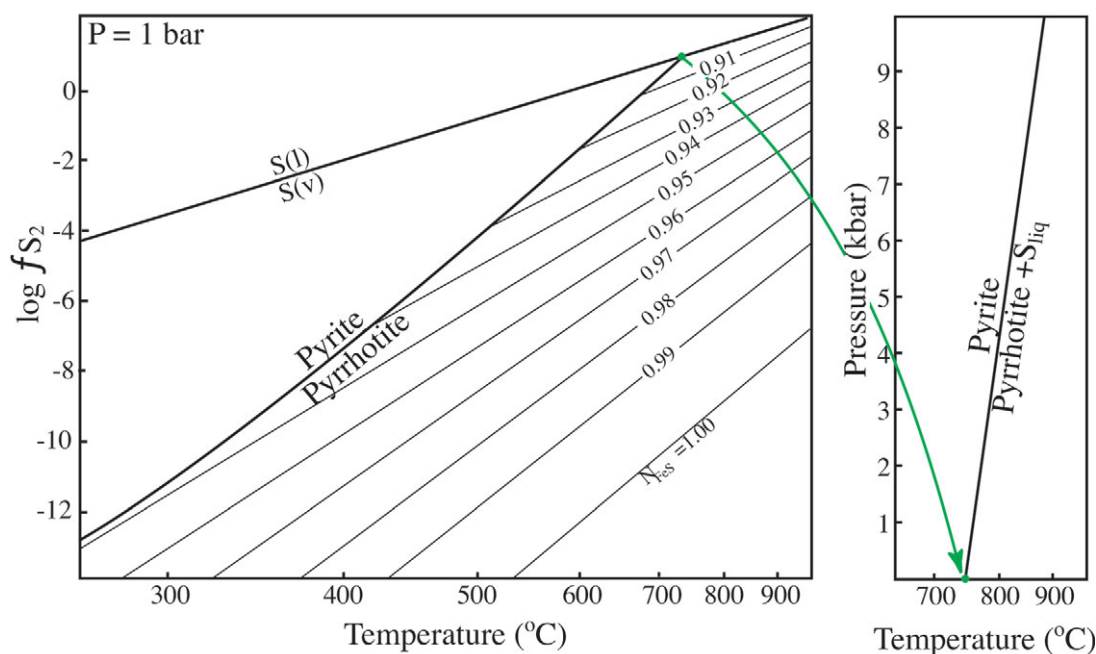
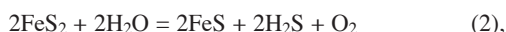


FIG. 1. $\log f(S_2)$ – temperature plot showing the stability of pyrite and pyrrhotite and the compositional variation of pyrrhotite. N_{FeS} is the mole fraction of FeS in pyrrhotite. Also shown is the limit of pyrite stability in P–T space. After Toulmin & Barton (1964) and Barker & Parks (1986).

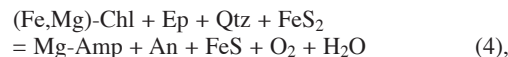
conditions are restricted to the pyrite–pyrrhotite curve while both minerals are in equilibrium. In general, prograde metamorphism of pyrite-rich rocks in a closed system will lead to formation of pyrrhotite and liberation of sulfur through reaction (1), thus driving up sulfur fugacity.

However, in natural rocks, two coupled processes compete with the $f(S_2)$ buffering effect of reaction (1). In one process, H_2O produced from metamorphically induced dehydration of silicates dissolves S and other components, leading to consumption of pyrite to maintain equilibrium proportions of H_2O , CO_2 , CH_4 , CO , O_2 , H_2 , H_2S , SO_2 and S_2 in the fluid (Connolly & Cesare 1993):

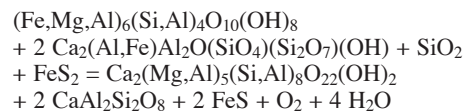


This process, which is insignificant at low temperatures owing to the low concentration of sulfur in metamorphic fluids on the Py–Po buffer, becomes increasingly significant as temperature rises, and is particularly applicable at low $f(O_2)$ conditions where high $X(H_2S)$ fluids can be generated (see Fig. 5d of Connolly & Cesare 1993).

In the second process, iron from silicates and oxides combines with the sulfur released from pyrite to form pyrrhotite (e.g., Tracy & Robinson 1988). This reaction is coupled to the first process in that hydrothermal fluids would facilitate interaction between sulfur and Fe-oxides and ferromagnesian silicates. Sulfur consumption is likely to be more effective where Fe is liberated through destruction of the silicate or oxide rather than through diffusion. This is the case with reactions involving oxides, which are consequently likely to be relatively efficient. Important silicate reactions include those where one ferromagnesian silicate is consumed to make another, for example:



or, rewritten with formulae,



Reactions such as (4) may be particularly effective at minimizing high $f(S_2)$ conditions because they involve the consumption of sulfur associated with both dehydration and sequestration of Fe from silicates. Many authors have also proposed that high $f(S_2)$ conditions may destabilize some ferromagnesian silicates (*e.g.*, Tracy & Robinson 1988).

There is some question concerning the metamorphic conditions at which Fe sequestration from silicates becomes relevant. Previous investigators of metamorphosed pyritic-graphitic sediments suggested that there is no noticeable sulfidation of silicates at 460–550°C and 3 kbar (Ferry 1981), whereas sulfidation becomes noticeable at ~540°C and 6 kbar (Nesbitt 1979), ~580°C and 6.6 kbar (Mohr & Newton 1983), and ~600°C and 5.5 kbar (Hutcheon 1979). At 650–725°C and 6 kbar, Tracy & Robinson (1988) noted clear evidence of extensive sulfidation of silicates. These authors used the Fe/(Fe + Mg) ratio of ferromagnesian silicates to monitor this process. Although the sulfidation of ferromagnesian silicates depends critically on fluid : rock ratios, such that every geological domain may behave differently, these previous studies do provide limited constraints on the metamorphic conditions required.

The consequence of these coupled sulfur-consuming processes is that in disseminated sulfide deposits, which may contain significant silicates or oxides of Fe and abundant H₂O-bearing silicates, pyrite can be completely consumed during metamorphism at moderate temperatures. On the other hand, disseminated sulfide deposits that initially lack these sulfur-scavenging reactants may preserve pyrite to higher metamorphic grades. Similarly, massive sulfide deposits that characteristically contain only sparsely distributed hydrous silicates and Fe-oxides and silicates may retain pyrite until high metamorphic temperatures are reached, resulting in high $f(S_2)$ conditions at mid-amphibolite facies and above. It is important to note that influx of an external hydrothermal fluid at amphibolite-facies conditions would result in pyrite consumption to maintain fluid equilibrium.

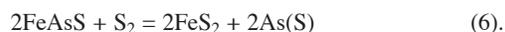
The system Fe–As–S

The stability field of arsenopyrite, in $\log f(S_2)$ – T space, is highlighted on Figure 2. This diagram also indicates the position of several metamorphic reactions that govern the formation and consumption of arsenopyrite. Each of the solid black diagonal lines on this diagram represents a desulfidation reaction, where sulfur is released by the reactant phases as temperature increases. The dashed bold line represents the boundary between regions where solid As (+ S) is stable and where As–S liquid is stable. Also shown on Figure 2 are the various paths that fluid composition may follow during metamorphism of arsenopyrite-bearing deposits. The paths and the reactions that control them are discussed in detail below.

Many types of ore deposits form through precipitation of sulfides in the stability field of arsenopyrite + pyrite. If, during metamorphism, sulfur is added to the chemical system, either through breakdown of another sulfur-bearing phase or through introduction of an external sulfur-rich fluid, the following incongruent reaction depicting arsenopyrite melting may occur (Path A, Fig 2):



Alternatively, if the initial temperature and $f(S_2)$ were low, the following reaction could take place:

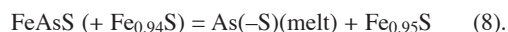


Other arsenopyrite-bearing deposits have a sulfide assemblage that is dominated by pyrite (\pm pyrrhotite) and contain sparse Fe as silicates or oxides. Once metamorphosed, such a deposit is likely to follow a $\log f(S_2)$ – T path similar to that indicated by Path B on Figure 2. In this case, pyrite breakdown on the Py–Po buffer leads to high $f(S_2)$ conditions that are eventually buffered beyond the stability field of arsenopyrite, leading to the following incongruent reaction of arsenopyrite melting:



At the boundary of individual crystals of arsenopyrite, the $\log f(S_2)$ – T path (starting from the black dot in the Py + Apy field on Fig. 2) may have a near-vertical trajectory initially, as arsenopyrite liberates sulfur during metamorphism, thereby increasing $f(S_2)$. The localized $\log f(S_2)$ – T path would thus intersect the curve for reaction (5), but instead of crossing the curve, sulfur liberation from arsenopyrite would buffer $f(S_2)$ along (5), towards the invariant reaction (7), where melting would take place. The position of reaction (7) in P – T space is shown in Figure 3. In comparing the position of this reaction with the $X(\text{H}_2\text{S})$ contents of metamorphic fluids (see Fig. 5d of Connolly & Cesare 1993), one can see that hydrothermal fluids do not contain significant amounts of sulfur when the reaction occurs. Therefore, reactions (2) and (3) do not consume enough pyrite to prevent reaction (7) in pyrite-rich rocks, unless a large amount of H₂O is produced or introduced. Sulfidation of Fe-oxides and ferromagnesian minerals (*e.g.*, reaction 4) may be more effective in consuming pyrite in natural rocks.

If all of the pyrite in a deposit initially containing pyrite + pyrrhotite + arsenopyrite is consumed during metamorphism before reaction (7) can take place, or if mineralization was precipitated in the stability field of arsenopyrite + pyrrhotite, another incongruent reaction of arsenopyrite melting is possible (Path C, Fig. 2):



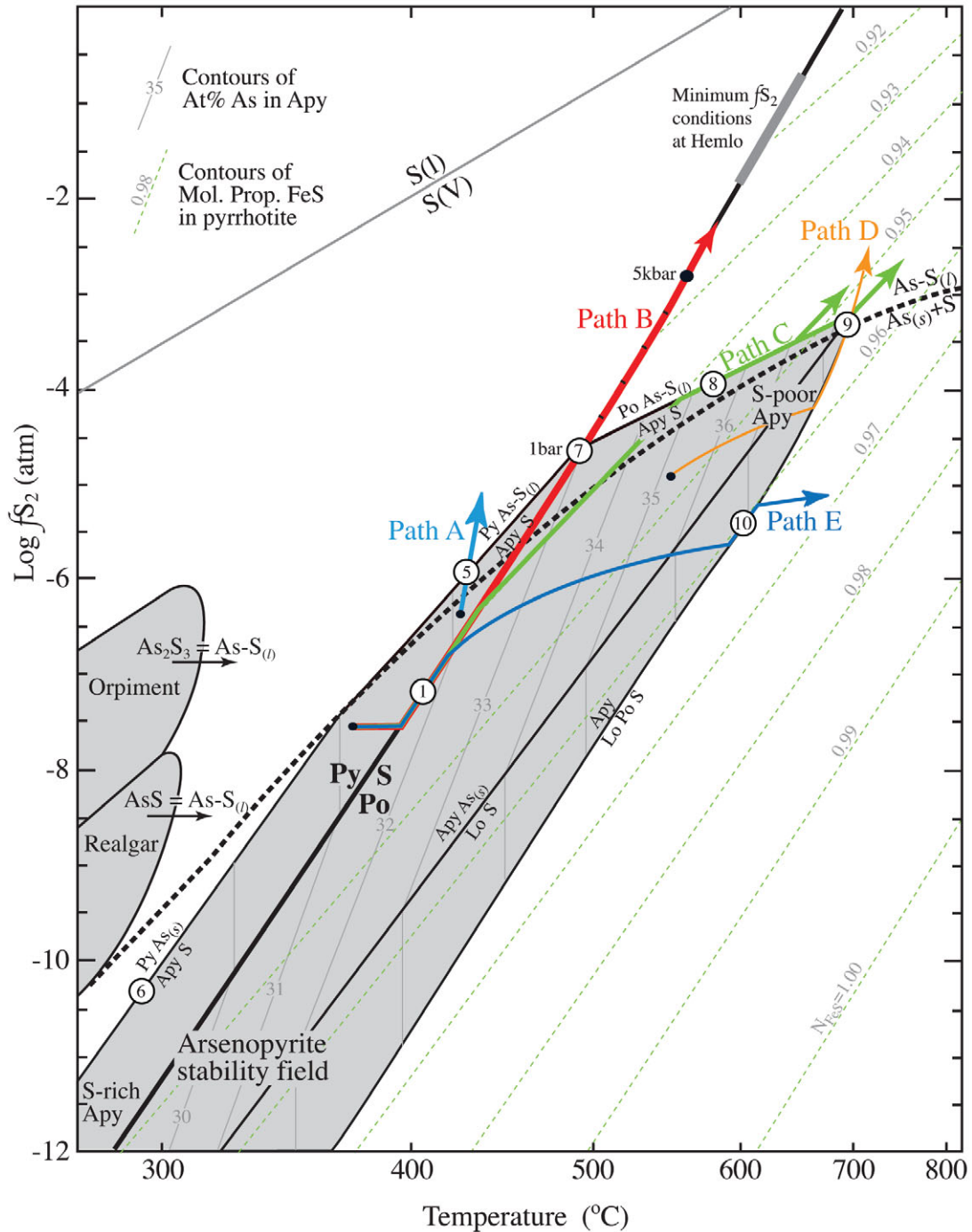


FIG. 2. $\text{Log } f_{\text{S}_2}$ – temperature grid showing the stability field of arsenopyrite, realgar and orpiment (grey shaded areas) and the position of the pyrite–pyrrhotite buffer (reaction 1). Original experimental work conducted by Barton (1969), 5 kbar pressure constraint determined by Sharp *et al.* (1985). The diagram also shows how f_{S_2} is buffered in various rocks, and how high f_{S_2} can lead to melting of arsenopyrite (explained in text). Note the position of the bold dashed curve, which divides the diagram into two fields; above this line As is only stable as a liquid (with sulfur) at moderate to high temperature, whereas below the line, it is stable as a solid.

This reaction (the stoichiometry of pyrrhotite is meant as an example only) may be a likely occurrence where arsenopyrite is hosted by massive to semimassive pyrrhotite. The liberation of S from pyrrhotite (the N_{FeS} isopleths of Fig. 2 indicate that pyrrhotite loses sulfur as temperature increases), as well as the continued desulfidation of arsenopyrite with increasing temperature, are likely to maintain a steep $\log f(\text{S}_2)$ -T trajectory that intersects the curve for reaction (8) in pyrrhotite-rich rocks (Path C, Fig. 2), provided that an external fluid is not introduced. Depending on the composition of coexisting pyrrhotite, reaction (8) may occur at temperatures between 491° and 702°C at 1 bar, or approximately 560° and 770°C at 5 kbar (Clark 1960a, Sharp *et al.* 1985).

However, reaction 8 is not enough to cause melting of all arsenopyrite that might be in the rock. Figure 4A shows that arsenic-sulfur melt requires slightly less than one mole of S for every mole of As. Because all sulfur required for the reaction comes from pyrrhotite, the $\log f(\text{S}_2)$ -T path must be buffered along the reaction (8) curve. Calculations indicate that from the 0.94 N_{FeS} isopleth to the 0.95 N_{FeS} isopleth, ~92 moles of pyrrhotite are required to melt one mole of arsenopyrite on the reaction (8) curve. In some massive sulfide deposits, ratios of pyrrhotite to arsenopyrite such as this or greater do occur. In these cases, the $\log f(\text{S}_2)$ -T path may track along the reaction (8) curve until arsenopyrite is consumed, at which point it will deviate upward on a track subparallel to the N_{FeS} isopleths again. In deposits lacking sufficient pyrrhotite, the $\log f(\text{S}_2)$ -T path will continue to track along the reaction (8) curve toward the invariant point at the upper stability-limit

of arsenopyrite. At this point the following incongruent melting reaction occurs:



The composition of the As-S melt that results from arsenopyrite melting through the various reactions is constrained by the phase relations illustrated in Figure 4A, which indicate the minimum sulfur content of the As-S melt over a range of temperatures. The melt composition is determined by the stoichiometry of the reactions. In each invariant-point melting reaction (7 and 9), the sulfur-rich pyrrhotite product requires slightly more sulfur than necessary for perfect stoichiometric ratios. Therefore, the As-S melt contains slightly less sulfur than a 1:1 sulfur to arsenic ratio. In this way, the melt composition may be buffered toward the minimum sulfur content, on the liquidus, indicated on Figure 4A.

If the original deposit contained arsenopyrite + pyrrhotite, but no pyrite, the following reaction may occur if there is insufficient pyrrhotite to buffer the sulfur fugacity to conditions required for reactions (8) and (9):



Liberation of sulfur by this reaction could theoretically buffer $f(\text{S}_2)$ (Path D, Fig. 2) to high enough conditions to reach the upper stability of arsenopyrite, causing melting through reaction (9). Along Path D, reactions (2) and (3) (or equivalents thereof, considering that arsenopyrite and not pyrite is the reactant in this case) are capable of overwhelming the positive $f(\text{S}_2)$ buffering effects of reaction (10). This may prevent reaction (9) from taking place in many rocks, particularly in disseminated deposits that follow a low $\log f(\text{O}_2)$ trajectory during metamorphism. In addition, it may not be possible for arsenopyrite hosted in massive pyrrhotite to generate a $\log f(\text{S}_2)$ -T trajectory steeper than the N_{FeS} isopleths of Figure 1 through reaction (10), because the additional sulfur generated would tend to be incorporated into pyrrhotite. Melting *via* reaction (9) along Path D might thereby be precluded in these rocks. Melting along Path D requires a low ratio of pyrrhotite to arsenopyrite, a lack of Fe silicates or oxides, and H_2O -deficient conditions, a combination that is probably rare.

Arsenopyrite is commonly found in orogenic gold deposits, where gold, arsenopyrite, pyrite or pyrrhotite (or both) were precipitated from a hydrothermal fluid at moderate temperatures, typically at or below the greenschist-amphibolite facies transition (~300 ± 50°C and 1–3 kbar, Groves *et al.* 1998). Many of these deposits are hosted in banded iron-formation (BIF) or mafic and ultramafic units, in which case the sulfides are associated with Fe-oxides and ferromagnesian silicates. During metamorphism of such rocks, pyrite is consumed at low temperatures, and then the relative

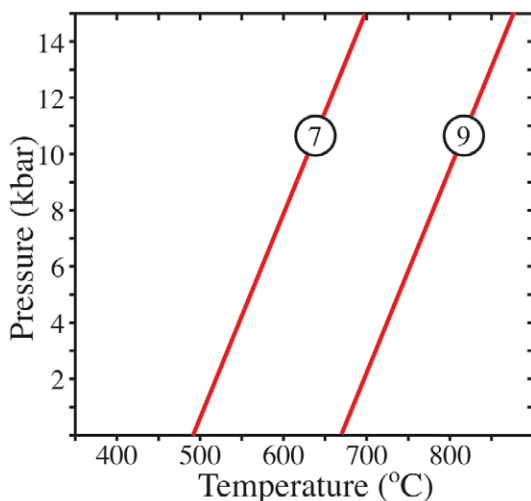
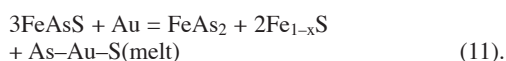


FIG. 3. A pressure - temperature diagram showing the positions of the two invariant reactions (7 and 9) describing the melting of arsenopyrite (from Clark 1960a).

sulfur fugacity falls owing to reactions such as (2–4). Ultimately, arsenopyrite starts to be converted to löllingite + pyrrhotite (Path E on Figure 2) through reaction (10). Note that reactions such as (2–4) are continuous along Path E, as sulfur is constantly liberated from both arsenopyrite and pyrrhotite during prograde metamorphism, leading to ongoing depletion of iron from Fe-oxides and ferromagnesian silicates. Any metamorphic fluid grows increasingly effective at incorporating sulfur. The extent to which the $\log f(\text{S}_2)$ -T trajectory follows reaction (10) depends upon the efficiency of sulfur sequestration by these processes, which in many rocks may lead to a löllingite + pyrrhotite assemblage at moderate temperatures without melting.

The system Au-Fe-As-S

Clark (1960a) found that where gold and arsenopyrite occur together, an Au-As-S melt forms by a modification of reaction (9):



Reaction (11) occurs at slightly lower temperatures than reaction (9). The $f(\text{S}_2)$ stability limits of this reaction are unknown. Given that Roland (1968) found 2 vol.% gold in Pb-As-S melt at 549°C, it is probable that some or all of the other arsenopyrite melting reactions are capable of incorporating gold in the melt if it is present.

Effects of element substitution in arsenopyrite

Arsenopyrite in many deposits contains Co and Ni in substitution for Fe, and also Sb in substitution for As. The presence of these elements is likely to affect the stability of arsenopyrite in the various reactions described above. In the case of Co and Ni, a range of binary alloy phase-diagrams indicate that these elements have a refractory behavior similar to that of Fe (see Massalski *et al.* 1990), implying that like Fe, they are unlikely to contribute significantly to the melt. Therefore, incongruent melting of intermediate and end-member phases in the system arsenopyrite – cobaltite – gersdorffite (FeAsS–CoAsS–NiAsS) is likely to produce As–S melt and solid sulfide phases such as pentlandite or cobalt-pentlandite in addition to pyrrhotite. These have been no experimental studies that show how the presence of Co or Ni affects the invariant melting reactions (7 and 9).

Experiments have shown that the mineral gudmundite (FeSbS), an end-member in the system FeAsS–FeSbS, is not stable beyond 280°C (Barton 1971), and breaks down at this temperature to form pyrrhotite and native antimony. Berthierite (FeSb₂S₄) starts to melt incongruently at 530°C (and it decomposes at 563°C) in the presence of pyrrhotite to form an Sb–S melt (Barton 1971). It is likely then that a small amount of

Sb substituting for As in arsenopyrite is not likely to greatly offset the melting temperature, and any such offset may be toward a lower temperature.

Summary

It is important to understand the above processes in order to interpret the behavior of arsenopyrite in natural occurrences. Within any one mineral deposit, arsenopyrite may undergo a range of different reactions during metamorphism depending on the local abundance and type of accompanying sulfide, silicate and oxide minerals. Although it may undergo melting in some areas, in others it may be preserved or undergo subsolidus metamorphism to löllingite + pyrrhotite.

RECOGNITION OF TEXTURES INDICATIVE OF AS-S MELT

Arsenopyrite melting should be considered as a possibility in any sulfide deposit that has been metamorphosed above the mid-amphibolite facies (>520°C, 2 kbar). Most rocks that have experienced this degree of metamorphism show signs of pervasive ductile deformation. Under these conditions, sulfide melts are highly mobile (Tomkins *et al.* 2004), so the ideal sites to investigate for evidence of As-bearing melts are structurally dilatant regions (such as boudin necks, extensional fractures, fold hinges and fault jogs) where mobile materials accumulate. Because As-bearing melts may persist to very low temperatures (Tomkins *et al.* 2004), even dilational structures that formed well after the peak of metamorphism may be sites of accumulation.

In studies of sulfide melts in igneous rocks, the occurrence of rounded nodules of sulfides (typically pyrrhotite, pentlandite and chalcopyrite) within mafic to ultramafic igneous rocks has been noted at many localities (Lightfoot *et al.* 1984, Naldrett 1984, Czamanske *et al.* 1992, Pritchard *et al.* 2004). These globular inclusions of sulfide are thought to form through immiscibility between silicate melt and sulfide melt. This is a very different physical environment to a much lower-temperature deforming solid metamorphic rock that contains a small amount of highly non-viscous sulfide melt. In the metamorphic environment, we do not expect to see large rounded nodular accumulations of sulfides. Instead, we expect that sulfide melts would mimic the shape of any dilational structural site (boudin necks, dilational fractures, *etc.*) because the tendency of the silicates, and particularly the melt, to deform under high strain would override the relatively minor surface-tension requirements of the molten sulfide to form a sphere. The best textural evidence that an assemblage was molten is that it occurs at a structurally dilatant site that formed at or near peak conditions of metamorphism (see Tomkins *et al.* 2004), though clearly this alone is not enough. Textural evidence of mobilization must be

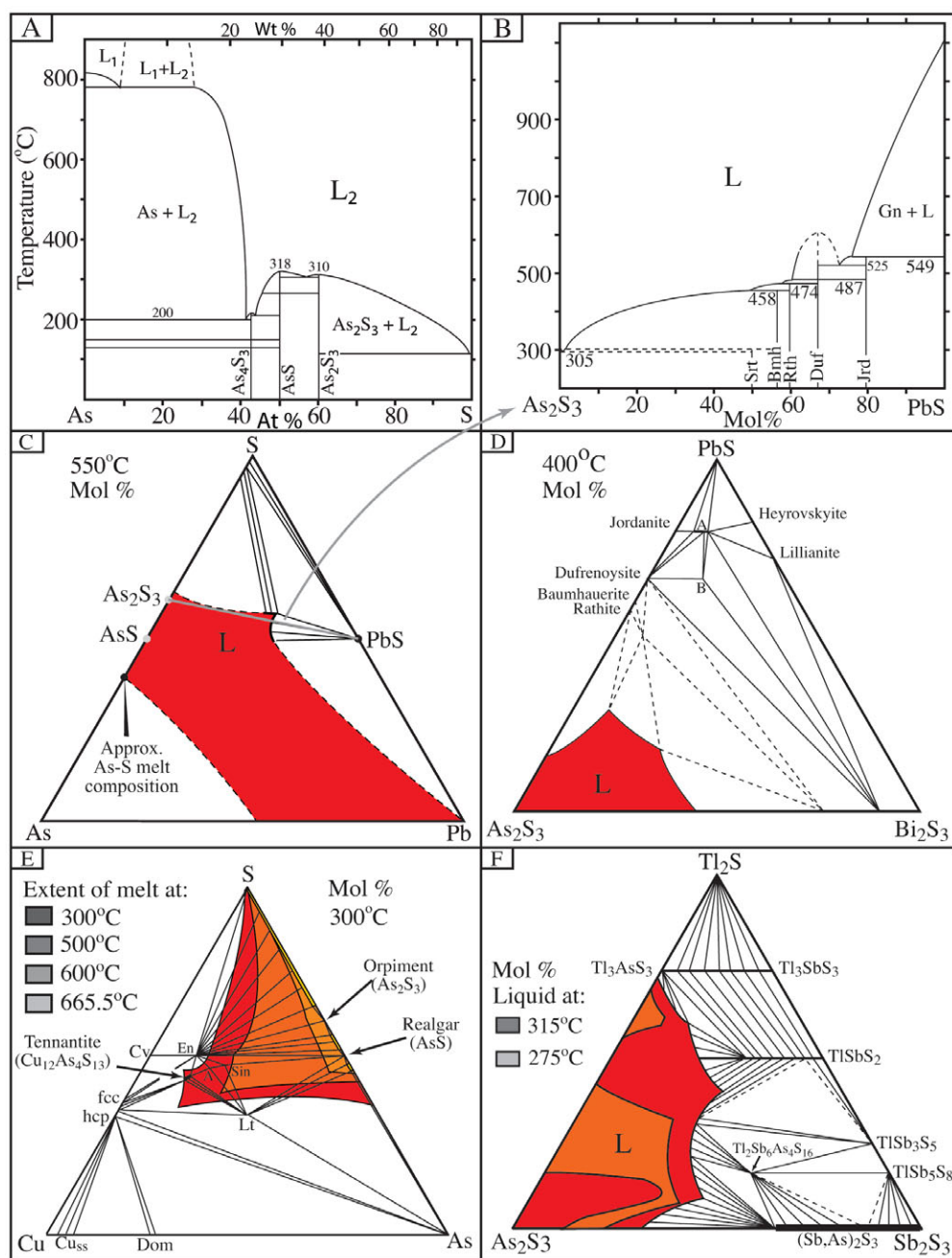


FIG. 4. Phase relations amongst As-bearing sulfosalts. (A) The system As-S (modified from Massalski *et al.* 1990). (B) The system As_2S_3 -PbS (modified from Kutolglu 1969). Here it is instructive to consider the effect of melting of a small proportion of arsenopyrite (to produce As-S melt) in the presence of galena. Symbols: Srt: sartorite, Bmh: baumhauerite, Rth: rathite, Duf: dufrenoyite, Jrd: jordanite. (C) The system As-Pb-S at 550°C [constructed from information in Roland (1968) and Massalski *et al.* (1990)] (D) The system As_2S_3 -PbS- Bi_2S_3 (after Walia & Chang 1973). (E) The system Cu-As-S (modified from Maske & Skinner 1971), showing the distribution of mineral phases and melt at 300°C, and the distribution of melt at 500°C, 600°C and 665.5°C. Symbols: Cv: covellite, En: enargite, A: unnamed compound, S: sinnerite, Lt: lautite, Dom: domeykite, fcc: face-centered cubic, hcp: hexagonal-closest packed. (F) The system As_2S_3 - Sb_2S_3 - Tl_2S (modified from Sobott 1984) showing phase distribution at 315°C (at 1 bar). The lightly shaded region represents the extent of the liquid field at 275°C.

coupled with experimental evidence that the mobilized assemblage would have been molten.

Arsenic–sulfur melts have the potential to cause significant melting of other sulfide and sulfosalt phases because they lower the melting temperature of a variety of these minerals, such that a range of elements can be incorporated in the melt at amphibolite-facies conditions (Fig. 4). Although they do not match exactly, As_2S_3 is considered a reasonable proxy for the actual composition of the As–S melt (see above) produced through arsenopyrite melting in these diagrams (*e.g.*, on Fig. 4C, one can see that a pseudobinary join drawn between the approximate As–S melt composition and PbS would produce almost the same topology as between As_2S_3 and PbS, which is shown in Fig. 4B; in the former, slightly more PbS would contribute to the melt). As has been shown at the Hemlo and Challenger gold deposits (Tomkins & Mavrogenes 2002, Tomkins *et al.* 2004), As-bearing melts readily incorporate and therefore mobilize gold. This is important because a high proportion of gold deposits contain appreciable disseminated arsenopyrite and pyrite. The high ratio of arsenopyrite to gold in these deposits implies that if an As–S melt is produced during metamorphism, it will melt much of the gold with which it comes in contact (if not all of it; see Roland 1968).

The presence of realgar or orpiment in and around dilational structures that formed approximately synchro-

nously with amphibolite-facies metamorphism (*e.g.*, Fig. 5A) is a clear indication of As-bearing melts, as these two minerals are molten beyond 318° and 310°C, respectively (at 1 bar; Fig. 2). Many other As-bearing sulfosalts are only stable at relatively low temperatures (Table 1), and their presence may similarly indicate that a melt existed in such rocks. In addition to the minerals listed in Table 1, many natural low-melting-point antimonian sulfosalts contain As in substitution for Sb (this is a characteristic of most sulfosalt minerals at the Hemlo deposit, as discussed below; see also Table 2).

If metamorphic grade and timing of mineralization are taken into consideration, several textures involving arsenopyrite may indicate crystallization of an As-bearing melt. (1) Pyrite–arsenopyrite intergrowths (Figs. 5B, E) may indicate the reversal of reaction (7), or possibly reaction (5) if another crystallizing phase requires S (*e.g.*, stibnite in Fig. 5B). (2) Pyrrhotite–arsenopyrite intergrowths may indicate the reversal of reaction (8). (3) Arsenopyrite intergrown with Fe-depleted sphalerite may indicate As–S melt + (Zn,Fe)S = FeAsS + ZnS. (4) Gold–arsenopyrite intergrowths (Fig. 5C; see Tomkins & Mavrogenes 2002, for detail) may indicate the reversal of reaction (11). Interpretation of these textures as crystallized As-bearing melts may be strengthened where other sulfides or sulfosalts coexist (Figs. 5B, D + E), where phase relations indicate that they would combine with an As–S melt. For

TABLE 1. MELTING TEMPERATURE OF ARSENIC-BEARING SULFOSALTS

Mineral Association	Formula	Melting temperature °C at 1 bar	Reference
Sartorite	$PbAs_2S_4$	305	Kutolglu (1969)
Orpiment	As_2S_3	310	Massalski <i>et al.</i> (1990)
Realgar	AsS	321	Massalski <i>et al.</i> (1990)
Baumhauerite	$Pb_2As_2S_9$	458	Kutolglu (1969)
Rathite	$(Pb,Tl)_2As_2S_{10}$	474	Kutolglu (1969)
Jordanite – Geochronite	$Pb_{14}(As,Sb)_6S_{23}$	549	Roland (1969)
Dufrénoysite	$Pb_2As_2S_5$	~600	Kutolglu (1969)
Tennantite	$Cu_{12}As_4S_{13}$	665	Maske & Skinner (1971)
Arsenopyrite	FeAsS	670	Clark (1960a)
Gersdorffite	NiAsS	Unknown	
Cobaltite	CoAsS	Unknown	
Parapirotite	$Tl(Sb,As)_2S_8$	Unknown	
Routhierite	$TlCu(Hg,Zn)_2(As,Sb)_2S_3$	Unknown	
Hutchinsonite	$(Pb,Tl)_2As_2S_6$	Unknown	
Chabournéite	$(Tl,Pb)_{21}(Sb,As)_9S_{147}$	Unknown	
Galkhaite	$(Cs,Tl)(Hg,Cu,Zn)_6(As,Sb)_4S_{12}$	Unknown	
Seligmannite	$PbCuAsS_5$	Unknown	
Paakkonenite	$Sb_7As_2S_2$	Unknown	
Aktashite	$Cu_4Hg_3As_4S_{12}$	Unknown	
Tvalchrelidzeite	$Hg_{12}(Sb,As)_8S_{15}$	Unknown	
Orpiment + Lorandite _{ss}	$As_2S_3 + Tl(Sb,As)_2S_2$	<275	Sobott (1984)
Lorandite + Stibnite	$TlAsS_2 + Sb_2S_3$	<275	Sobott (1984)
Orpiment + Galena	$As_2S_3 + PbS (>44\% As_2S_3)$	~300	Kutolglu (1969)
Orpiment + Stibnite	$As_2S_3 + Sb_2S_3$	<310	Tomkins <i>et al.</i> (2004)
Orpiment + Bismuthinite	$As_2S_3 + Bi_2S_3 (>30\% As_2S_3)$	<310	Walia & Chang (1973)
Arsenopyrite + Pyrite	$FeAsS + FeS_2$	491	Clark (1960a)
Native As + Au	As + Au	636	Hansen & Anderko (1958)

TABLE 2. RESULTS OF ELECTRON-MICROPROBE ANALYSES OF MINERALS FROM HEMLO, CHALLENGER, MONTAUBAN, OSBORNE LAKE AND GECO DEPOSITS

Deposit Sample	Hemlo			Challenger			Montauban			Osborne Lake			Geco													
	UC	Hem	Hem	AGT	AGT	AGT	Mnt	Au-Ag	Fiz	Os	Cp	Gn	Sel	Po	Gn	Owy?	Td	Cp	Bi	Apy						
14636	013b	015e	014	024	034	011				35-40								020								
Mineral	Apy	Stc	Py	Rlg	Apy	Au	Po	Dys	Apy	Gn	Au-Ag	Fiz	Mineral	Apy	Tn	Cp	Gn	Sel	Po	Gn	Owy?	Td	Cp	Bi	Apy	
S mass %	20.60	28.39	52.73	20.66	18.33	-	39.48	0.90	20.11	13.13	0.16	19.35	S mass %	20.42	28.51	35.09	12.20	19.78	39.37	13.16	15.75	19.91	34.42	0.00	21.04	
As	41.79	1.81	0.05	60.27	47.13	-	0.01	0.00	41.15	0.00	0.00	0.00	As	41.17	17.88	0.00	0.00	10.29	0.03	0.00	0.00	0.00	0.02	0.00	0.00	39.21
Sb	0.03	69.94	0.00	0.76	-	-	-	23.05	0.10	1.02	0.61	32.16	Sb	0.00	1.74	0.00	0.00	6.45	0.00	0.02	4.49	25.98	0.01	1.95	2.84	
Pb	0.00	0.00	0.00	0.00	-	-	-	0.00	0.00	82.70	0.00	38.24	Pb	0.00	0.00	0.00	82.65	44.25	0.00	82.76	39.49	0.00	0.00	0.00	0.18	
Cu	0.01	0.01	0.00	0.00	-	0.06	0.00	0.03	0.00	0.02	0.00	0.14	Cu	0.51	43.50	34.35	1.25	13.35	0.03	0.00	0.94	13.46	33.60	0.02	1.12	
Ag	0.00	0.00	0.03	0.06	-	1.70	-	58.68	0.03	0.45	39.90	6.19	Ag	0.00	0.19	0.01	0.11	0.00	0.03	1.26	2.32	32.00	0.00	0.05	0.02	
Au	0.00	0.08	0.00	0.00	-	98.27	59.95	14.80	0.00	0.00	57.15	0.00	Au	0.02	0.03	0.00	0.00	0.00	0.05	0.00	0.00	0.00	0.00	0.00	0.00	
Fe	35.99	0.25	46.42	0.00	31.54	-	0.00	0.02	34.09	0.01	-	0.03	Fe	35.17	5.58	30.51	0.26	1.62	60.28	0.01	0.17	5.76	29.07	0.00	34.76	
Co	-	-	-	-	1.26	-	0.24	-	-	-	-	-	Co	-	-	-	-	-	-	-	-	-	-	-	-	
Ni	-	-	-	-	0.89	-	-	-	-	-	-	-	Ni	-	-	-	-	-	-	-	-	-	-	-	-	
Bi	-	-	-	-	-	-	-	-	-	-	-	-	Bi	-	-	-	-	-	-	0.00	34.94	0.07	0.07	98.22	0.00	
Zn	0.00	0.06	0.03	0.00	-	-	0.28	-	-	-	-	-	Zn	0.05	2.14	0.08	0.00	0.00	0.00	0.00	-	-	-	0.01	0.00	
Hg	0.15	0.27	0.09	0.28	-	0.00	-	-	-	-	-	-	Hg	-	-	-	-	-	-	-	-	-	-	-	0.00	
Total	98.57	100.82	99.35	82.03	99.15	100.03	99.96	97.47	95.48	97.83	97.83	96.13	Total	97.33	99.58	100.05	96.49	95.74	99.80	97.21	98.09	97.18	97.20	100.25	99.17	
S at. %	34.82	59.33	66.22	44.14	31.72	-	53.23	3.35	35.08	49.85	0.76	54.26	S at. %	34.90	45.33	50.14	47.28	48.97	53.19	49.94	53.11	42.94	50.55	0.00	35.58	
As	30.22	1.62	0.03	55.10	34.91	-	0.01	0.00	30.72	0.00	0.00	0.00	As	30.11	12.17	0.00	0.00	10.90	0.02	0.00	0.00	0.00	0.01	0.00	28.38	
Sb	0.01	38.48	0.00	0.43	-	-	-	22.61	0.04	1.02	0.75	23.73	Sb	0.00	0.73	0.00	0.00	4.21	0.00	0.02	3.98	14.75	0.01	3.29	1.26	
Pb	0.00	0.00	0.00	0.00	0.00	-	-	0.00	0.00	48.57	0.00	16.59	Pb	0.00	0.00	0.00	49.55	16.95	0.00	48.59	20.60	0.00	0.00	0.00	0.04	
Cu	0.01	0.02	0.00	0.00	-	0.18	0.00	0.05	0.00	0.04	0.00	0.20	Cu	0.44	34.90	24.77	2.45	16.68	0.02	0.00	1.60	14.65	24.90	0.07	0.95	
Ag	0.00	0.00	0.01	0.04	-	3.06	-	64.98	0.02	0.51	55.19	5.16	Ag	0.00	0.09	0.01	0.13	0.00	0.01	1.42	2.32	20.50	0.00	0.09	0.01	
Au	0.00	0.03	0.00	0.00	-	96.76	-	8.98	0.00	0.00	43.30	0.00	Au	0.01	0.01	0.00	0.00	0.00	0.01	0.00	0.00	0.00	0.00	0.00	0.00	
Fe	34.91	0.30	33.46	0.00	31.35	-	46.41	0.04	34.14	0.01	-	0.05	Fe	34.51	5.10	25.03	0.58	2.30	46.75	0.02	0.33	7.13	24.51	0.00	33.75	
Co	-	-	-	-	-	-	0.00	-	-	-	-	-	Co	-	-	-	-	-	-	-	-	-	-	-	-	
Ni	-	-	-	-	0.84	-	0.18	-	-	-	-	-	Ni	-	-	-	-	-	-	-	-	-	-	-	-	
Bi	0.00	0.00	0.00	0.00	-	-	-	-	-	0.00	-	-	Bi	-	-	-	-	-	-	0.00	18.07	0.02	0.02	96.52	0.00	
Zn	0.00	0.06	0.02	0.00	-	-	0.19	-	-	-	-	-	Zn	0.04	1.67	0.05	0.00	0.00	0.00	0.00	-	-	-	-	0.03	
Hg	0.04	0.09	0.02	0.10	-	0.00	-	-	-	-	-	-	Hg	-	-	-	-	-	-	-	-	-	-	-	0.00	
Total	100	100	100	100	100	100	100	100	100	100	100	100	Total	100	100	100	100	100	100	100	100	100	100	100	100	100

* The analysis of realgar produced a low total owing to the volatility of this mineral, which destabilizes in the beam. Its identity was confirmed by reflected light microscopy. Mineral symbols used: Apy: arsenopyrite, Bi: native bismuth, Cp: chalcopyrite, Dys: dyscrasite, Gn: galena, Fiz: fizeflyite, Au: gold, Au-Ag: gold-silver alloy, Owy: owyheite, Py: pyrite, Po: pyrrhotite, Rlg: realgar, Sel: seligmannite, Ste: sibirite, Tn: tennantite, Td: tetrahedrite.

example, in the sample from Hemlo (Fig. 5B), arsenopyrite is associated with stibnite + realgar (+ several other rarer sulfosalts), a combination that melts well below the 600–650°C of peak metamorphism at Hemlo (Powell *et al.* 1999, Tomkins *et al.* 2004). Confidence that a sulfosalts–arsenopyrite association formed through crystallization of a metal–As–S melt may be strengthened where sulfosalts containing low-melting-point chalcophile elements (LMCE: Sb, Bi, Tl, Sn, Cd, Hg, Au and Ag; Frost *et al.* 2002a) are significantly more abundant than elsewhere (as is the case in Fig. 5F).

AN EXAMPLE OF MELTING AT HIGH SULFUR FUGACITY: PATH A: THE HEMLO GOLD DEPOSIT

Background

The Hemlo deposit, in central Ontario, Canada, is one of the world's largest gold deposits and has an enigmatic mineral assemblage analogous with both epithermal- and porphyry-style mineralization; it has thus far evaded widely accepted categorization (*e.g.*, Muir 2002). Most recent authors (see Tomkins *et al.* 2004) consider it to be a premetamorphic gold deposit that was metamorphosed at 600–650°C and 6–7 kbar (Powell *et al.* 1999). The deposit contains abundant evidence for the existence of an Sb–As-rich melt during peak metamorphism (Tomkins *et al.* 2004). The As component of this melt could theoretically have come from breakdown of realgar or orpiment (or both) if mineralization was originally introduced at low temperatures (<~318°C, depending on pressure). However, disseminated arsenopyrite is preserved in strained wallrocks at Hemlo (Harris 1989), suggesting that the premetamorphic conditions of mineralization (Fig. 2) were beyond the stability of realgar and orpiment (molten realgar or orpiment would have been mobilized from such rocks). Thus, arsenopyrite is the most likely As-bearing reactant phase for generation of the As-rich melt within the orebody.

The following observations of the Hemlo mineralization serve as the basis for our discussion. (1) The majority of host rocks are pyrite-rich and poor in Fe silicates and oxides. Only a minor biotite-rich metabasic rock contains an appreciable amount of Fe in silicates and oxides. (2) Arsenopyrite is relatively common in the hanging-wall rocks, where it is the principal mineral of arsenic, yet it is rare within the ore zones (Harris 1989). Where it does occur in the ore zones, it is more prevalent in biotite-rich zones (Harris 1989). Within the felsic and pelitic units (*i.e.*, units poor in Fe oxides and ferromagnesian silicates), we have observed arsenopyrite only in dilational structural domains, where polymetallic melts accumulated, and where it is intimately associated with pyrite and sulfosalts (Fig. 5B). (3) The sulfur-bearing mineral assemblage throughout the deposit is dominated by pyrite, barite and molybdenite (Harris 1989), to the extent that these are the only sulfur-bearing minerals

that are abundant and widespread throughout the deposit. Pyrrhotite and magnetite are rare within the ore zones, occurring mainly in biotite-rich rocks, whereas in the hanging-wall rocks, they are comparatively common (Harris 1989). (4) Barian K-feldspar and barian mica are widely distributed throughout the deposit (Harris 1989). Most barian K-feldspar grains show consistent concentric zoning, with wide zones of low-Ba core and high-Ba margin (Fig. 4C in Tomkins *et al.* 2004). These typically display a granoblastic texture with ~120° triple-junctions, and intervening material is commonly restricted to triple junctions. Grain boundaries of barian silicates and small fractures therein have anomalous Ba contents.

Factors controlling arsenopyrite melting at Hemlo

The fact that large amounts of pyrite are preserved within the Hemlo deposit indicates that high $f(S_2)$ conditions must have prevailed during peak metamorphism. The highlighted region on the pyrite–pyrrhotite buffer curve (Fig. 2) represents the actual $f(S_2)$ conditions in rocks containing pyrrhotite + pyrite, and the minimum $f(S_2)$ conditions in rocks lacking pyrrhotite. Although there are a number of other desulfidation reactions that buffer $f(S_2)$ (*e.g.*, Seal *et al.* 1990), many of these are likely to have been localized and short-lived at Hemlo because most of the minerals involved are relatively uncommon. Conversely, because pyrite, barite and molybdenite dominate the sulfur-bearing mineral assemblage at Hemlo, reactions involving these minerals are expected to have had the most widespread influence on $f(S_2)$.

In the absence of significant Fe silicates and oxides, reaction (1) is capable of raising $f(S_2)$ beyond the stability of arsenopyrite, leading to melting through reaction (7). However, both reactions (1) and (7) produce pyrrhotite, of which there is a distinct lack in many parts of the deposit, suggesting that arsenopyrite did not melt on the Py–Po buffer. Alternative explanations of arsenopyrite melting require the consumption of a widespread S-bearing mineral within the stability field of pyrite and at sulfur fugacities above the pyrite–pyrrhotite buffer (*i.e.*, reaction 5). The assemblage molybdenite + pyrite is stable up to ~750°C (Grover *et al.* 1975), so the only abundant mineral capable of keeping the system at high $f(S_2)$, off the Py–Po buffer, is barite. The observations listed above support the notion of barite instability during metamorphism, particularly the ~120° triple-junctions among zoned barian K-feldspar grains. Furthermore, the anomalous Ba contents along microfractures within barian K-feldspar indicate continued late mobility of barium.

These observations suggest a variable stability of barite with increasing temperature, and not simply instability of barite during the hydrothermal reaction(s) that introduced mineralization. An example of how barite might be consumed during progressive metamorphism

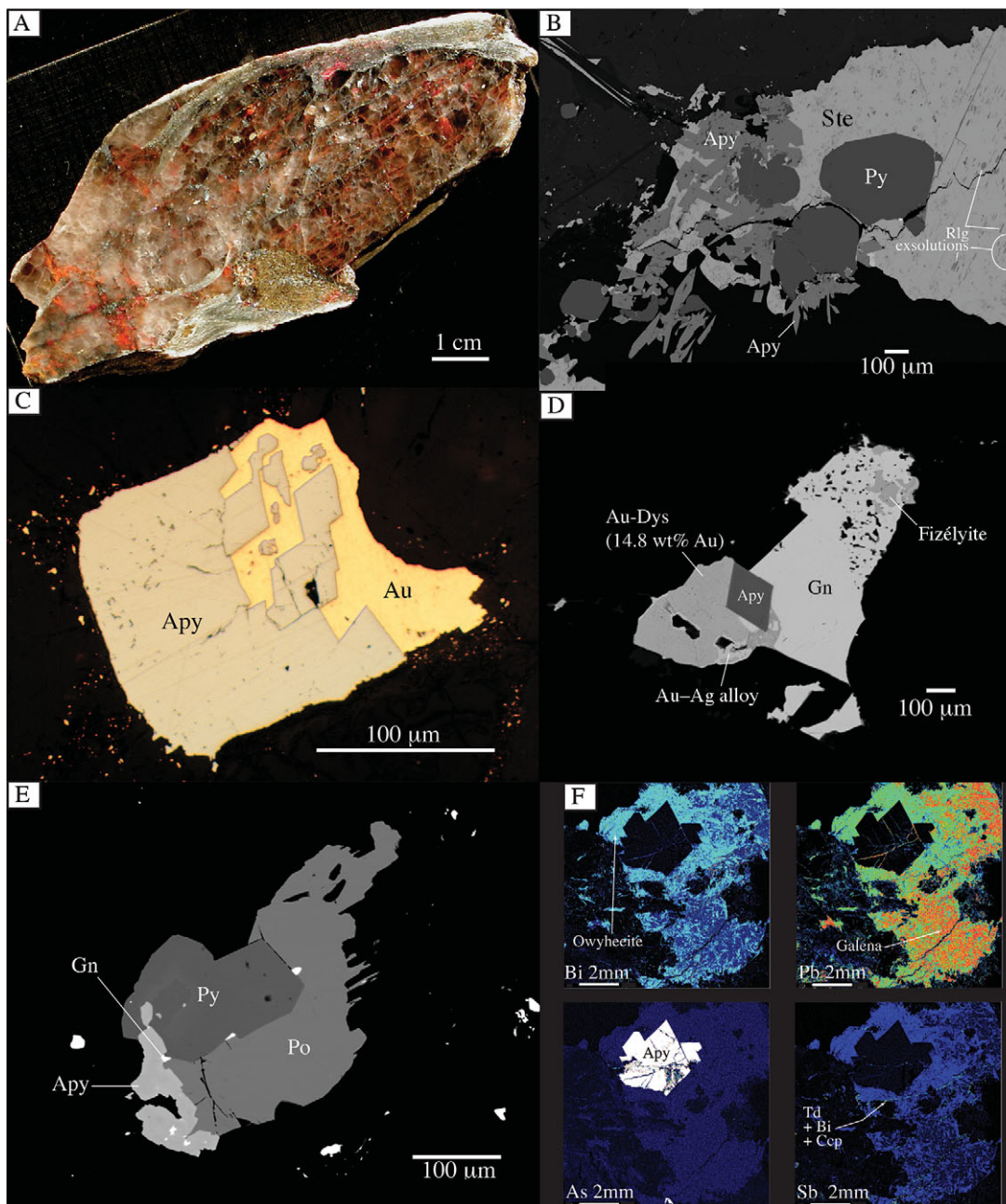
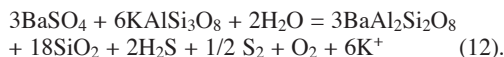


FIG. 5. Examples of textures and mineral associations that may indicate that an As-bearing melt was generated during metamorphism (if considered together with metamorphic grade and timing of mineralization). Symbols: Apy: arsenopyrite, Py: pyrite, Po: pyrrhotite, Gn: galena, Ste: stibnite, Rlg: realgar, Dys: dyscrasite, Td: tetrahedrite, Ccp: chalcopyrite. (A) Photograph of part of a boudinaged quartz vein from the Hemlo gold deposit, interpreted to have been deformed approximately synchronously with peak metamorphism, involving temperatures of 600–650°C (Tomkins *et al.* 2004). Brightness and contrast have been enhanced to highlight the realgar (AsS), which appears orange and red. Realgar ($T_m = 318^\circ\text{C}$; Massalski *et al.* 1990), together with stibnite and many other sulfosalts, were concentrated in dilational structures in and around many similar features at Hemlo (Tomkins *et al.* 2004). (B) BSE image of an intergrowth of arsenopyrite and pyrite within a boudinaged feldspar vein from Hemlo. This may represent the reversal of reaction (5), as there is no pyrrhotite in most rocks at Hemlo.

to produce Ba-enriched K-feldspar is given by the following reaction:



Other reactions are possible, depending on assumptions about element mobility. Note that this reaction is both an oxidizing and a desulfidation reaction. Through this and similar mechanisms of barite consumption, we anticipate conditions of increasing $f(\text{S}_2)$ during progressive metamorphism, favoring conditions within the stability field of pyrite throughout much of the Hemlo deposit (Fig. 2). In a study on barite-rich rocks 21 km to the west of Hemlo, Pan & Fleet (1991) similarly suggested that barium in muscovite and feldspars came from the adjacent barite-rich units during peak metamorphism.

In the biotite-rich metamafic unit, reactions similar to reaction (4) are expected to have maintained conditions of lower $f(\text{S}_2)$, thus ensuring the persistence of arsenopyrite. Similarly, in the hanging wall, where pyrrhotite and magnetite are more abundant, the diminished amount of pyrite (the pyrite present now may be retrograde) is expected to have led to lower $f(\text{S}_2)$ conditions during peak metamorphism, allowing preservation of arsenopyrite.

Also present is stibnite with abundant exsolution-induced blebs of realgar ($T_m < 556^\circ\text{C}$; Tomkins *et al.* 2004). (C) Photomicrograph of an arsenopyrite–gold inclusion from the Challenger gold deposit. An experiment on an offcut of this rock showed that similar arsenopyrite–gold inclusions melted at P–T conditions below those estimated at Challenger ($T_{\text{metam}} = 800\text{--}850^\circ\text{C}$; Tomkins & Mavrogenes 2002). (D) BSE image showing an association between arsenopyrite and galena from the Montauban Zn–Pb–Au deposit ($T_{\text{metam}} = \sim 650^\circ\text{C}$; Jourdain 1993). Also present are Au-bearing dyscrasite (Ag_3Sb ; $T_m = 558^\circ\text{C}$; Hanson & Anderko 1958), Au–Ag alloy and fizélyite ($\text{Pb}_{14}\text{Ag}_5\text{Sb}_{21}\text{S}_{48}$; $T_m = \text{unknown}$), and linking many similar associations are veinlets of pyrrargyrite (Ag_3SbS_3 ; $T_m = 485^\circ\text{C}$; Bryndzia & Kleppa 1988). (E) BSE image showing an association between arsenopyrite, pyrite and pyrrhotite (minor galena) from the same sample as (D), which we consider likely to represent the reversal of reaction (7). (F) Element-distribution maps of Bi, Pb, As and Sb, showing an association between arsenopyrite, galena and Bi-rich owyheite [$\text{Pb}_7\text{Ag}_2(\text{Sb},\text{Bi})_8\text{S}_{20}$; $T_m = \text{unknown}$] from the Geco Zn–Cu deposit ($600^\circ < T_{\text{metam}} < 700^\circ\text{C}$; Peterson & Zaleski 1999). Also present are minor amounts of Ag-rich tetrahedrite [$(\text{Ag},\text{Cu})_{10}(\text{Cu},\text{Fe},\text{Zn})_2(\text{Sb},\text{As})_4\text{S}_{13}$; $T_m \approx 485^\circ\text{C}$; Bryndzia & Kleppa 1988], native Bi ($T_m = 271^\circ\text{C}$; *e.g.*, Massalski *et al.* 1990) and chalcopyrite. Mineral compositions confirmed using WDS analysis on the JEOL JXA8200 electron microprobe at the University of Calgary (Table 2) and reflected light microscopy.

EXAMPLES OF ARSENOPYRITE MELTING ON THE PY–PO BUFFER: PATH B: CANADIAN VMS DEPOSITS

To study arsenopyrite melting on the Py–Po buffer (reaction 7), we investigated several Canadian massive Pb–Zn sulfide deposits that were metamorphosed at conditions of the middle to upper amphibolite facies. The Geco deposit in central Ontario was metamorphosed at $600\text{--}700^\circ\text{C}$ and 3–6 kbar (Peterson & Zaleski 1999), the Montauban deposit in central Quebec, at $\sim 650^\circ\text{C}$ and 5 kbar (Jourdain 1993), and the Osborne Lake deposit in western Manitoba, at $\sim 700^\circ\text{C}$ and 6 kbar (*cf.* Bristol & Froese 1989, Kraus & Menard 1997). These are all considered to be volcanogenic massive sulfide (VMS) deposits, and arsenopyrite melting at Osborne Lake has already been postulated by Frost *et al.* (2002b). Although each deposit is characterized by massive sulfides, there are significant differences among them. At Geco, the massive sulfide assemblage is dominated by pyrite, pyrrhotite, sphalerite and chalcopyrite, and there is typically <1% galena in the ore (Friesen *et al.* 1982) and only sparse arsenopyrite. Montauban is characterized by massive sphalerite, galena, chalcopyrite, pyrite and pyrrhotite, and has marginal disseminated gold-rich sulfide mineralization (Stamatelopoulos-Seymour & MacLean 1984, Bernier *et al.* 1987); again, arsenopyrite is only sparsely distributed. Osborne Lake, conversely, contains relatively common arsenopyrite amongst massive pyrrhotite, pyrite (euhedral crystals locally exceeding 10 cm), sphalerite and chalcopyrite; galena is rare (Bristol & Froese 1989).

Each deposit contains both pyrite and pyrrhotite, and the pyrite is commonly euhedral, which suggests some retrograde growth on the Py–Po buffer, as is typical of highly metamorphosed massive sulfides (Craig & Vokes 1993). There is also evidence that pyrite persisted through peak metamorphism in that old cores, some with Co zonation and some without, are commonly found within euhedral pyrite [Fig. 6A; see Craig & Vokes (1993), for a discussion of similar cores]. The cores with oscillatory Co zoning are interpreted to represent remnants of the original hydrothermal mineralization event, with the alternating zones possibly representing fluctuations in fluid chemistry; these are less likely to be mimicked by slow metamorphic growth (*e.g.*, Shore & Fowler 1996). If so, pyrite was stable throughout the history of the deposits, and $f(\text{S}_2)$ conditions were on the Py–Po buffer during peak metamorphism in many parts of the deposits. Given that the peak conditions of metamorphism estimated for each deposit are beyond the temperature required for reaction (7), arsenopyrite probably melted, if it was present in these high- $f(\text{S}_2)$ regions. In combination with the phase relations, the textures depicted in samples from Montauban, Geco and Osborne Lake suggest that arsenopyrite melting may have occurred at each deposit (Figs. 5, 6).

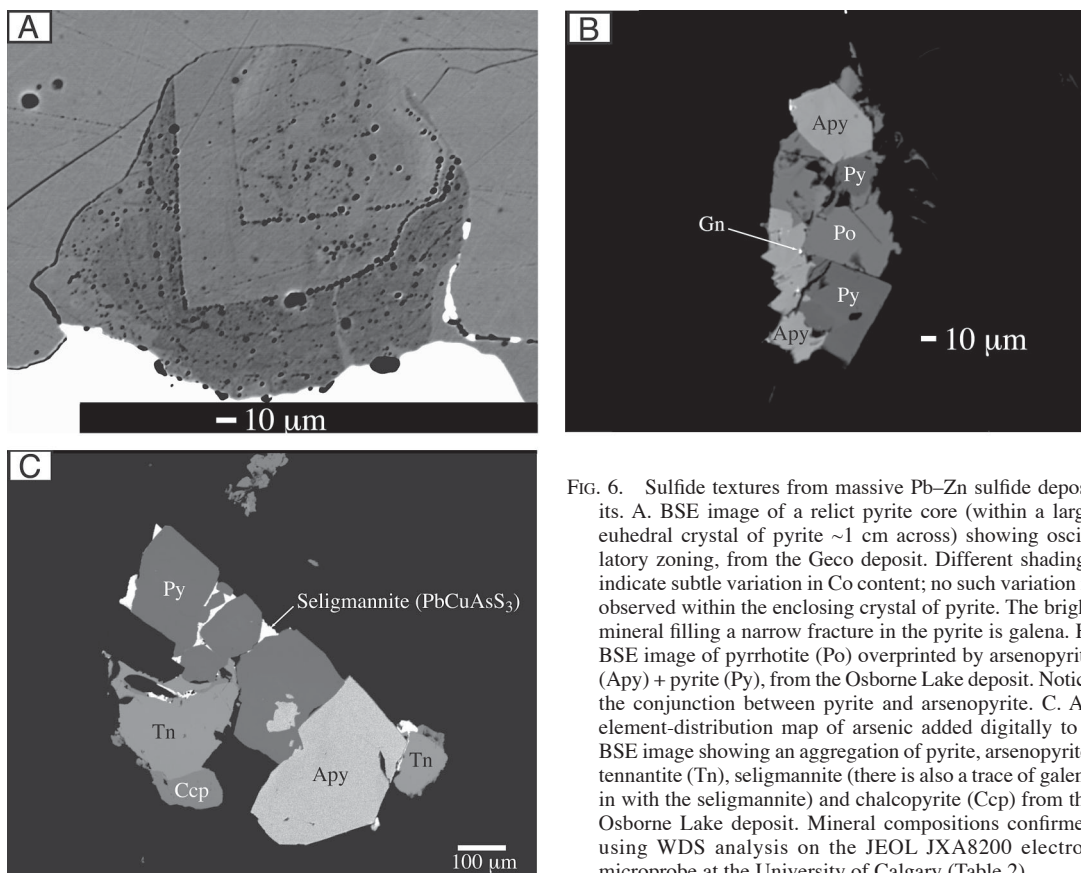


FIG. 6. Sulfide textures from massive Pb–Zn sulfide deposits. A. BSE image of a relict pyrite core (within a large euhedral crystal of pyrite ~1 cm across) showing oscillatory zoning, from the Geco deposit. Different shadings indicate subtle variation in Co content; no such variation is observed within the enclosing crystal of pyrite. The bright mineral filling a narrow fracture in the pyrite is galena. B. BSE image of pyrrhotite (Po) overprinted by arsenopyrite (Apy) + pyrite (Py), from the Osborne Lake deposit. Notice the conjunction between pyrite and arsenopyrite. C. An element-distribution map of arsenic added digitally to a BSE image showing an aggregation of pyrite, arsenopyrite, tennantite (Tn), seligmannite (there is also a trace of galena in with the seligmannite) and chalcopyrite (Ccp) from the Osborne Lake deposit. Mineral compositions confirmed using WDS analysis on the JEOL JXA8200 electron microprobe at the University of Calgary (Table 2).

Figures 5D and E from Montauban are from the same sample; it contains numerous similar sulfide–sulfosalt aggregations, as well as microveinlets of pyrrargyrite linking many of them, within a thin layer in a quartz–feldspathic rock. Many of the sulfosalts that coexist with arsenopyrite in this sample melt at temperatures (T_m) well below the peak temperature of metamorphism at Montauban, for example pyrrargyrite ($T_m = 485^\circ\text{C}$, Bryndzia & Kleppa 1988) and dyscrasite ($T_m = \sim 558^\circ\text{C}$, Hanson & Anderko 1958). Others, particularly galena, are sulfides that are known to melt in the presence of As–S melts (Fig. 4B). The sulfide–sulfosalt aggregations are also highly enriched in Sb, Ag and Au relative to all other rocks in the deposit, all of which partition strongly into sulfide melts (Mavrogenes *et al.* 2001, Tomkins *et al.* 2004). There is also a lack of sphalerite, which is abundant in the massive sulfides, but which is known to be a refractory sulfide that does not contribute strongly to sulfide melts (Mavrogenes *et al.* 2001, Tomkins *et al.* 2004). These observations suggest that the sulfide–sulfosalt aggregations in this sample represent a mobilized As-bearing polymetallic melt,

which was probably derived in part through melting of arsenopyrite *via* reaction (7).

Figure 5F, from the Geco deposit, is a good example of the problematics in establishing whether an observed assemblage was molten. The sulfide–sulfosalt material in this example occurs within a fracture in granitic wallrock adjacent to massive sulfides, and there is a moderate amount of alteration to muscovite associated with it. The muscovite might suggest that the assemblage formed as a consequence of hydrothermal mobilization from the massive sulfides. However, there are indications the assemblage was molten, and because hydrothermal fluids and sulfide melts migrate into the same structurally dilatant sites during deformation, it is possible that the alteration and mineralization are unrelated. The main observation that suggests sulfide melt mobilization rather than hydrothermal mobilization is that the mineral assemblage in question contains S, Pb, As, Bi, Cu, Sb and Ag, but little Fe and no Zn. The assemblage is strongly enriched in LMCE and depleted in Fe and Zn relative to the massive sulfides, a feature characteristic of sulfide melt extracted from

its residue. Neither hydrothermal nor solid-state mobilization produces this characteristic fractionation, so sulfide melt mobilization is the favored explanation. It is difficult to rule out the alternative possibility that the observed assemblage was hydrothermally introduced from an external source and completely unrelated to the adjacent massive sulfides.

Figures 6B and 6C are examples from Osborne Lake. These figures show textural relationships among arsenopyrite, sulfides and sulfosalts within a fracture cutting a fragment of a quartz vein. This quartz vein fragment is presumed to be premetamorphic because ductile deformation of massive sulfides typically breaks up and mills any enclosed competent lithologies during prograde or peak deformation. There were no clearly postmetamorphic quartz veins at Osborne Lake. The fragmented vein was sampled specifically because (1) dilational microfractures commonly develop in competent lithologies during deformation into which mobile components (such as melt) migrate, and (2) the separation of any melt accumulations from large quantities of galena eliminates an exsolution origin for the sulfosalts. Figure 6B shows arsenopyrite + pyrite overgrowing pyrrhotite; this is an unstable assemblage at peak conditions of metamorphism. This texture is consistent with reaction between As–S melt and pyrrhotite (reversal of reaction 7) during cooling. Figure 6C shows a similar intergrowth involving pyrite, chalcopyrite and several As-bearing minerals including arsenopyrite, tennantite and seligmannite (PbCuAsS_3), again within a fracture transecting a quartz vein. The tennantite contains appreciable Sb and Ag, which, as indicated above, tend to be concentrated in sulfide melts. In addition to arsenopyrite, tennantite ($T_m = 665^\circ\text{C}$ at 1 bar, Fig. 4E) and possibly seligmannite (T_m is unknown) may also be unstable at the peak conditions of metamorphism, in which case this texture may represent a cooling reaction between an As–Cu–Pb–Sb–Ag–S melt and pyrrhotite. Although these textures suggest that some arsenopyrite at the Osborne Lake mine melted during peak metamorphism, there are also examples throughout the deposit which suggest that arsenopyrite survived peak metamorphism in some localities, such as very coarse euhedral crystals of arsenopyrite in textural equilibrium with pyrrhotite in the absence of pyrite. Although this texture could simply reflect a reversal of reaction (8), these arsenopyrite crystals do not appear to be concentrated in dilational structures and do not have rare sulfosalts associated with them.

ARSENOPYRITE STABILITY-RELATIONS IN LOW-SULFUR ENVIRONMENTS: PATH E: METAMORPHOSED IRON FORMATIONS

There are many iron-formation-hosted gold deposits, with attendant arsenopyrite, that can be investigated to gain an understanding of the premetamorphic assemblage and its expected evolution during metamorphism.

In addition, we have shown that arsenopyrite stability is governed by pyrite-breakdown reactions in most rocks, so we can examine the fate of pyrite in metamorphosed iron-formations to gauge whether arsenopyrite would melt or be preserved.

In BIF-hosted gold deposits in Archean greenstone belts around the world, mineralization is generally thought to have been introduced during or slightly after peak metamorphism. The gold is typically associated with disseminated pyrrhotite and arsenopyrite, with pyrite usually absent or rare (see *e.g.*, Phillips *et al.* 1984, Smith 1996, Mueller 1997, Neumayr *et al.* 1998), although there are examples with significant pyrite (*e.g.*, Vearncombe 1986). If such a deposit becomes metamorphosed, for example during a second cycle of orogenesis, melting of arsenopyrite is unlikely to occur for several reasons. Where pyrite is absent, two mechanisms are capable of raising sulfur fugacity. One involves liberation of small amounts of sulfur from disseminated pyrrhotite as temperature increases (Fig. 2). A second involves consumption of arsenopyrite (which is typically only a minor component) through reaction (10), leaving less of it to melt if high enough $f(\text{S}_2)$ conditions are reached. The abundant Fe oxides and silicates in iron formations are likely to inhibit rising sulfur fugacity through reactions similar to reaction (4), especially as temperatures rise toward the $>700^\circ\text{C}$ necessary for arsenopyrite melting through reaction (9). Even in deposits that do contain pyrite prior to metamorphism, reactions similar to reaction (4) are likely to sufficiently suppress rising $f(\text{S}_2)$, such that neither of reactions (7), (8) or (9) can proceed.

The Geco deposit (discussed above) and Calumet deposit (Quebec, Canada) provide useful natural laboratories with which to compare the extent of pyrite consumption during metamorphism of iron formation *versus* massive sulfide. Like Geco, Calumet is thought to be a VMS deposit that was metamorphosed at $650\text{--}700^\circ\text{C}$ and 4–6 kbar (Williams 1990). At Geco, massive sulfides are part of a stratigraphic sequence that includes sulfidic iron formation, and at Calumet sulfidic magnetite-rich layers also are preserved. At both areas, each of these units likely contained pyrite as part of the initial assemblage deposited in a subaqueous environment. Whereas the massive sulfide bodies at both mines preserve a significant proportion of pyrite as well as pyrrhotite (Fig. 7A), the magnetite-rich layers now contain abundant pyrrhotite and some sphalerite, but only sparse retrograde pyrite (Fig. 7B). Within the massive sulfides, sulfur fugacity was driven up along the pyrite–pyrrhotite buffer as metamorphism progressed because there were no competing reactions that consumed sulfur. In these areas, arsenopyrite melting might be expected given the high peak temperature (Fig. 5F shows assemblages that support arsenopyrite melting at Geco; no arsenic minerals were found at Calumet). In contrast, all pyrite in the iron formation was consumed during metamorphism, and high $f(\text{S}_2)$ conditions were

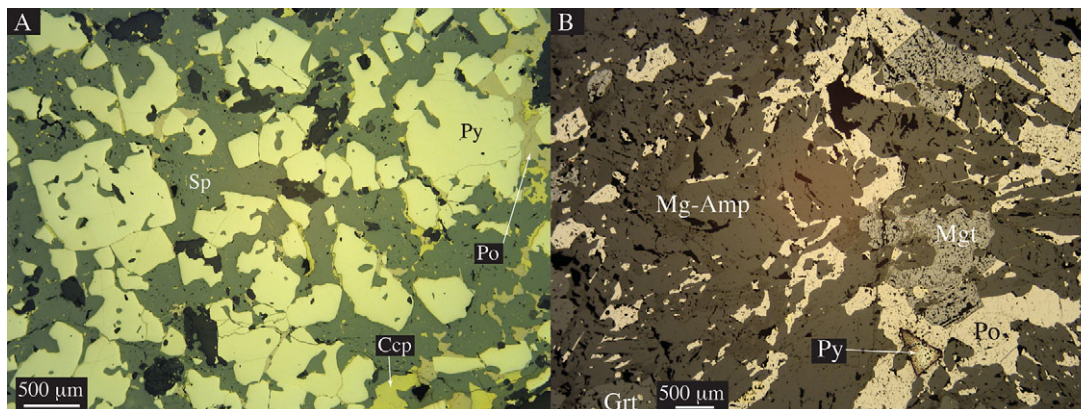


FIG. 7. Differing contents of pyrite in two rocks of approximately the same metamorphic grade. A. Abundant anhedral to euhedral pyrite (Py) in massive sulfides, with sphalerite (Sp), pyrrhotite (Po) and chalcopyrite (Ccp). From the Geco deposit. B. Minor euhedral (therefore probably retrograde) pyrite amongst abundant disseminated pyrrhotite within a garnet (Grt) + magnetite (Mgt) + Mg-amphibole (anthophyllite–gedrite) matrix. From the Calumet deposit. Mineral compositions confirmed using WDS analysis on the JEOL JXA8200 electron microprobe at the University of Calgary and reflected light microscopy.

never reached. In these regions, arsenopyrite (if it ever existed) would be expected to be either preserved or converted to pyrrhotite + löllingite (reaction 10).

CONCLUSIONS

Although melting of arsenopyrite may play a role in the melting of ore deposits during metamorphism, the tendency for arsenopyrite to melt is dependent on reactions in the surrounding the rock and the evolution of sulfur fugacity. In most mineral deposits, the likelihood that it will melt, or instead be transformed into löllingite + pyrrhotite, depends upon the durability of pyrite. Where pyrite remains within the rock beyond ~560°C (at 5 kbar; 491°C at 1 bar), $f(S_2)$ is buffered to high levels, and arsenopyrite will melt by reaction (7). In deposits with disseminated sulfides and moderately abundant Fe-bearing silicates and oxides, arsenopyrite is unlikely to melt because pyrite is more easily converted to pyrrhotite at relatively low temperatures in such rocks, precluding buffering of $f(S_2)$ to the level required for reaction (7). Arsenopyrite that occurs in pyrrhotite-rich massive sulfides may melt by reactions (8) and (9), provided that the system remains closed to external fluids during progressive metamorphism. In summary, arsenopyrite-bearing massive Pb–Zn deposits and some disseminated gold deposits may be the most likely to experience arsenopyrite melting and generation of a multi-element sulfide melt capable of segregating ore metals, particularly gold and silver, through deformation-induced mobilization.

ACKNOWLEDGEMENTS

We thank in particular Eva Zaleski and Susan Swapp for help in obtaining access and collecting samples from the Geco and Osborne Lake mines, respectively, as well as useful discussions pertinent to this paper. John MacLachy is thanked for providing access to drill core and geological information about the Calumet deposit. Jean Bernard was very helpful in giving a tour of the Montauban deposit and assisting with selecting drill-core samples. The assistance of Hugh Lockwood and Dave Truscott at the Golden Giant mine, and Gord Skrecky at the Williams mine, in viewing the Hemlo orebody and obtaining samples is greatly appreciated. Mark Smyk of the Ontario Geological Survey is also thanked for providing samples from Hemlo and Geco. We also thank Tom Heine of the Manitoba Geological Survey for help in sampling the Osborne Lake mine. We appreciate the efforts of Eric Essene and an anonymous reviewer who greatly helped to improve the manuscript. Funding for this project was provided by an Alberta Ingenuity Fellowship to A.G.T., NSF grant EAR-0125113 to B.R.F., and NSERC Discovery Grant 037233 to D.R.M.P.

REFERENCES

- BARKER, W.W. & PARKS, T.C. (1986): The thermodynamic properties of pyrrhotite and pyrite; a re-evaluation. *Geochim. Cosmochim. Acta* **50**, 2185-2194.
- BARTON, P.B., JR. (1969): Thermochemical study of the system Fe–As–S. *Geochim. Cosmochim. Acta* **33**, 841-857.

- BARTON, P.B., JR. (1971): The Fe–Sb–S system. *Econ. Geol.* **66**, 121-132.
- BERNIER, L., POULIOT, G. & MACLEAN, W.H. (1987): Geology and metamorphism of the Montauban north gold zone: a metamorphosed polymetallic exhalative deposit, Grenville Province, Quebec. *Econ. Geol.* **82**, 2076-2090.
- BRISTOL, C.C. & FROESE, E. (1989): Highly metamorphosed altered rocks associated with the Osborne Lake volcanogenic massive sulfide deposit, Snow Lake area, Manitoba. *Can. Mineral.* **27**, 593-600.
- BRYNDZIA, L.T. & KLEPPA, O.J. (1988): High-temperature reaction calorimetry of solid and liquid phases in the quasi-binary system $\text{Ag}_2\text{S}-\text{Sb}_2\text{S}_3$. *Geochim. Cosmochim. Acta* **52**, 167-176.
- CLARK, L.A. (1960a): The Fe–As–S system: phase relations and applications. *Econ. Geol.* **55**, 1345-1381 (Part I).
- CLARK, L.A. (1960b): The Fe–As–S system: phase relations and applications. *Econ. Geol.* **55**, 1631-1652 (Part II).
- CONNOLLY, J.A.D. & CESARE, B. (1993): C–O–H–S fluid composition and oxygen fugacity in graphitic metapelites. *J. Metam. Geol.* **11**, 379-388.
- CRAIG, J.R. & VOKES, F.M. (1993): The metamorphism of pyrite and pyritic ores: an overview. *Mineral. Mag.* **57**, 3-18.
- CZAMANSKE, G.K., KUNILOV, V.Y., ZIENTEK, M.L., CABRI, L.J., LIKHACHEV, A.P., CALK, L.C. & OSCARSON, R.L. (1992): A proton-microprobe study of magmatic sulfide ores from the Noril'sk–Talnakh district, Siberia. *Can. Mineral.* **30**, 249-287.
- FERRY, J.M. (1981): Petrology of graphitic sulfide-rich schists from south-central Maine: an example of desulfidation during prograde regional metamorphism. *Am. Mineral.* **66**, 908-930.
- FRIESEN, R.G., PIERCE, G.A. & WEEKS, R.M. (1982): Geology of the Geco base metal deposit. In *Precambrian Sulfide Deposits* (R.W. Hutchinson, C.D. Spence & J.M. Franklin, eds.). *Geol. Assoc. Can., Spec. Pap.* **25**, 343-363.
- FROST, B.R., MAVROGENES, J.A. & TOMKINS, A.G. (2002a): Partial melting of sulfide ore deposits during medium- and high-grade metamorphism. *Can. Mineral.* **40**, 1-18.
- FROST, B.R., SWAPP, S.M. & HEINE, T.H. (2002b): Partial melting of massive sulfide ore bodies in the Snow Lake District, Manitoba. *Geol. Assoc. Can. – Mineral. Assoc. Can., Program Abstr.* **27**, 37.
- GROVER, B., KULLERUD, G. & MOH, G.H. (1975): Phase equilibrium conditions in the ternary Fe–Mo–S system in relation to natural minerals and ore deposits. *Neues Jahrb. Mineral., Abh.* **124**, 246-272.
- GROVES, D.I., GOLDFARB, R.J., GEBRE-MARIAM, M., HAGEMANN, S.G. & ROBERT, F. (1998): Orogenic gold deposits: a proposed classification in the context of their crustal distribution and relationship to other gold deposit types. *Ore Geol. Rev.* **13**, 7-27.
- HANSON, M. & ANDERKO, K. (1958): *Constitution of Binary Alloys*. McGraw-Hill, New York, N.Y.
- HARRIS, D.C. (1989): The mineralogy and geochemistry of the Hemlo gold deposit, Ontario. *Geol. Surv. Can., Econ. Geol. Rep.* **38**.
- HOFMANN, B.A. (1994): Formation of a sulfide melt during Alpine metamorphism of the Lengenbach polymetallic sulfide mineralization, Bintal, Switzerland. *Mineral. Deposita* **29**, 439-442.
- HUTCHEON, I. (1979): Sulfide–oxide–silicate equilibria, Snow Lake, Manitoba. *Am. J. Sci.* **279**, 643-665.
- JOURDAIN, V. (1993): *Géologie des Amas Sulfurés Aurifères de la Province de Grenville*. Thèse de doctorat, Université du Québec à Montréal, Montréal, Canada.
- KRAUS, J. & MENARD, T. (1997): A thermal gradient at constant pressure: implications for low- to medium-pressure metamorphism in a compressional tectonic setting, Flin Flon and Kiseynew domains, Trans-Hudson Orogen, central Canada. *Can. Mineral.* **35**, 1117-1136.
- KRETSCHMAR, U. & SCOTT, S.D. (1976): Phase relations involving arsenopyrite in the system Fe–As–S and their application. *Can. Mineral.* **14**, 364-386.
- KUTOLGLU, A. (1969): Röntgenographische und thermische Untersuchungen im quasibinären System $\text{PbS}-\text{As}_2\text{S}_3$. *Neues Jahrb. Mineral., Monatsh.*, 68-72.
- LIGHTFOOT, P.C., NALDRETT, A.J. & HAWKESWORTH, C.J. (1984): The geology and geochemistry of the Waterfall Gorge section of the Insizwa Complex with particular reference to the origin of nickel sulfide deposits. *Econ. Geol.* **79**, 1857-1879.
- MASKE, S. & SKINNER, B.J. (1971): Studies of the sulfosalts of copper. I. Phases and phase relations in the system Cu–As–S. *Econ. Geol.* **66**, 901-918.
- MASSALSKI, T.B., OKAMOTO, H., SUBRAMANIAN, P.R. & KACPRZAK, L., eds. (1990): *Binary Alloy Phase Diagrams* (2nd edition). American Society for Metals, Metals Park, Ohio.
- MAVROGENES, J.A., MACINTOSH, I.W. & ELLIS, D.J. (2001): Partial melting of the Broken Hill galena–sphalerite ore: experimental studies in the system $\text{PbS}-\text{FeS}-\text{ZnS}-(\text{Ag}_2\text{S})$. *Econ. Geol.* **96**, 205-210.
- MOHR, D.W. & NEWTON, R.C. (1983): Kyanite–staurolite metamorphism in sulfidic schists of the Anakeesta Formation, Great Smoky Mountains, North Carolina. *Am. J. Sci.* **283**, 97-134.
- MUELLER, A.G. (1997): The Nevoria gold skarn deposit in Archean iron-formation, Southern Cross Greenstone Belt,

- Western Australia. I. Tectonic setting, petrography, and classification. *Econ. Geol.* **92**, 181-209.
- MUIR, T.L. (2002): The Hemlo gold deposit, Ontario, Canada: principal deposit characteristics and constraints on mineralization. *Ore Geol. Rev.* **21**, 1-66.
- NALDRETT, A.J. (1984): The Ni-Cu ores of the Sudbury Igneous Complex: mineralogy and composition of the Sudbury ores. In *The Geology and Ore Deposits of the Sudbury Structure* (E.G. Pye, A.J. Naldrett & P.E. Giblin, eds.). *Ont. Geol. Surv., Spec. Vol. 1*, 309-325.
- NESBITT, B.E. (1979): *Regional Metamorphism of the Ducktown, Tennessee, Massive Sulfides and Adjoining Portions of the Southern Blue Ridge Province*. Ph.D. thesis, Univ. of Michigan, Ann Arbor, Michigan.
- NEUMAYR, P., RIDLEY, J.R., MCNAUGHTON, N.J., KINNY, P.D., BARLEY, M.E. & GROVES, D.I. (1998): Timing of gold mineralisation in the Mt York district, Pilgangoora greenstone belt, and implications for the tectonic and metamorphic evolution of an area linking the western and eastern Pilbara Craton. *Precamb. Res.* **88**, 249-265.
- PAN, YUANMING & FLEET, M.E. (1991): Barian feldspar and barian-chromian muscovite from the Hemlo area, Ontario. *Can. Mineral.* **29**, 481-498.
- PETERSON, V.L. & ZALESKI, E. (1999): Structural history of the Manitowadge greenstone belt and its volcanogenic Cu-Zn massive sulfide deposits, Wawa subprovince, south-central Superior Province. *Can. J. Earth Sci.* **36**, 606-625.
- PHILLIPS, G.N., GROVES, D.I. & MARTYN, J.E. (1984): An epigenetic origin for Archean banded iron-formation-hosted gold deposits. *Econ. Geol.* **79**, 162-171.
- POWELL, W.G., PATTISON, D.R.M. & JOHNSTON, P. (1999): Metamorphic history of the Hemlo gold deposit from Al₂SiO₅ mineral assemblages, with implications for the timing of mineralization. *Can. J. Earth Sci.* **36**, 33-46.
- PRITCHARD, H.M., HUTCHINSON, D. & FISHER, P.C. (2004): Petrology and crystallization history of multiphase sulfide droplets in a mafic dike from Uruguay: implications for the origin of Cu-Ni-PGE sulfide deposits. *Econ. Geol.* **99**, 365-376.
- ROLAND, G.W. (1968): The system Pb-As-S. *Mineral. Deposita* **3**, 249-260.
- SEAL, R.R., II, ESSENE, E.J. & KELLY, W.C. (1990): Tetrahedrite and tennantite: evaluation of thermodynamic data and phase equilibria. *Can. Mineral.* **28**, 725-738.
- SHARP, Z.D., ESSENE, E.J. & KELLY, W.C. (1985): A re-examination of the arsenopyrite geothermometer: pressure considerations and applications to natural assemblages. *Can. Mineral.* **23**, 517-534.
- SHORE, M. & FOWLER, A.D. (1996): Oscillatory zoning in minerals; a common phenomenon. *Can. Mineral.* **34**, 1111-1126.
- SMITH, D.S. (1996): Hydrothermal alteration at the Mineral Hill mine, Jardine, Montana: a lower amphibolite facies Archean lode gold deposit of probable synmetamorphic origin. *Econ. Geol.* **91**, 723-750.
- SOBOTT, R.J.G. (1984): Sulfosalts and Ti₂S-As₂S₃-Sb₂S₃-S phase relations. *Neues Jahrb. Mineral., Abh.* **150**, 54-59.
- STAMATELOPOULOU-SEYMOUR, K. & MACLEAN, W.H. (1984): Metamorphosed volcanogenic ores at Montauban, Grenville Province, Quebec. *Can. Mineral.* **22**, 595-604.
- TOMKINS, A.G. & MAVROGENES, J.A. (2002): Mobilization of gold as a polymetallic melt during pelite anatexis at the Challenger gold deposit, South Australia: a metamorphosed Archean deposit. *Econ. Geol.* **97**, 1249-1271.
- TOMKINS, A.G., PATTISON, D.R.M. & ZALESKI, E. (2004): The Hemlo gold deposit, Ontario: an example of melting and mobilization of a precious metal - sulfosalt assemblage during amphibolite facies metamorphism and deformation. *Econ. Geol.* **99**, 1063-1084.
- TOULMIN, P., III & BARTON, P.B., JR. (1964): A thermodynamic study of pyrite and pyrrhotite. *Geochim. Cosmochim. Acta* **28**, 641-671.
- TRACY, R.J. & ROBINSON, P. (1988): Silicate - sulfide - oxide - fluid reactions in granulite-grade pelitic rocks, central Massachusetts. *Am. J. Sci.* **288A**, 45-74.
- VEARNCOMBE, J.R. (1986): Structure of veins in a gold-pyrite deposit in banded iron formation, Amalia Greenstone Belt, South Africa. *Geol. Mag.* **123**, 601-609.
- WALIA, D.S. & CHANG, L.L.Y. (1973): Investigations in the systems PbS-Sb₂S₃-As₂S₃ and PbS-Bi₂S₃-As₂S₃. *Can. Mineral.* **12**, 113-119.
- WILLIAMS, P.J. (1990): The gold deposit at Calumet, Quebec (Grenville Province): an example of the problem of metamorphic versus metamorphosed ore. In *Regional Metamorphism of Ore Deposits* (P.G. Spry & L.T. Bryndzia, eds.). Coronet Books, Utrecht, The Netherlands (1-25).

Received February 22, 2005, revised manuscript accepted April 9, 2006.